

Enhancing the High Voltage XLPE Cable Insulation Characteristics Using Functionalized TiO₂ Nanoparticles

Abdelrahman Said¹, Amira Gamal Nawar^{1,2,*}, Elsayed Alaa Eldesoky³, Samir Kamel⁴, Mousa Awdallah Abd-Allah¹

¹Electrical Engineering Department, Shoubra Faculty of Engineering, Benha University, Cairo, Egypt

²Higher Institute for Engineering and Modern Technology, Marg, Cairo, Egypt

³Polymer and Pigment Department, National Research Centre, Giza, Egypt

⁴Cellulose and Paper Department, National Research Centre, Giza, Egypt

Email address:

abdelrahman.ghoniem@feng.bu.edu.eg (A. Said), eng_amira.2009@yahoo.com (A. G. Nawar), alaa_chemist@yahoo.com (E. A. Eldesoky), samirki@yahoo.com (S. Kamel), mousa_abdullah@yahoo.co (M. A. Abd-Allah)

*Corresponding author

To cite this article:

Abdelrahman Said, Amira Gamal. Nawar, Elsayed Alaa. Eldesoky, Samir Kamel, Mousa Awdallah. Abd-Allah. Enhancing the High Voltage XLPE Cable Insulation Characteristics Using Functionalized TiO₂ Nanoparticles. *American Journal of Polymer Science and Technology*. Vol. 6, No. 3, 2020, pp. 21-31. doi: 10.11648/j.ajpst.20200603.11

Received: August 30, 2020; **Accepted:** September 14, 2020; **Published:** October 13, 2020

Abstract: The current research aims to study the influence of loading Titanium Dioxide (TiO₂) nanoparticles on the dielectric, thermal and mechanical properties of the commercial Cross-Linked Polyethylene (XLPE) used as the main insulation in power cables. Using the concept of composite, XLPE/TiO₂ nanocomposites samples were prepared by the melt blending method with different ratios of nanoparticles (0.5, 2, 3.5 and 5% wt/wt). The surface treatment of TiO₂ nanoparticles was carried out to reduce the agglomeration of TiO₂ nanoparticles inside the XLPE. The morphology of the prepared samples was studied by X-ray Diffraction (XRD) and the dispersion of nanoparticles in the XLPE polymer matrix is checked using Field Emission Scanning Electron Microscopy (FE-SEM). Thermal analysis test for all samples have been investigated. The dielectric properties, such as dielectric constant (ϵ_r) and loss tangent ($\tan \delta$) for XLPE/TiO₂ nanocomposites were measured under frequencies ranging from 1 Hz to 1 MHz. AC Breakdown Voltage (AC-BDV) was also measured using a controlled high voltage testing transformer (50 Hz) under sphere-to-sphere field. The mechanical properties were evaluated by performing the tensile test and tensile strength and elongation values were measured. It was found that nanocomposites with functionalized TiO₂ exhibited better dielectric, thermal and mechanical properties compared to nanocomposites with nonfunctionalized TiO₂.

Keywords: XLPE, Nanocomposites, Titanium Nanoparticles, Electrical, Thermal, and Mechanical Properties

1. Introduction

The excellent characteristics of polymers, such as reliability, availability, low cost, light weight, easy fabrications, and appropriate processing ability, support their using as the main insulation in high voltage cables [1]. Polyethylene (PE) is the most important polyolefin type because of its superior properties; since it is a semi-crystalline polymer with a low cost and easy to manufacture and fabricate. Moreover, it has a wide array of engineering properties such as toughness, low coefficient of friction, chemical corrosion, and high resistance, and near-zero moisture absorption [2]. All these unique

characteristics resulted in an ideal material for many applications especially in electrical insulation. Crosslinked Polyethylene (XLPE) is one shape from PE shapes. These polymers are widely used as electrical insulating materials; however, their high properties can be reduced over time due to different aging processes such as exposure to heat, humidity and mechanical stress [3-5]. So, there is still a need to further develop the insulation properties of these materials. One method for enhancing polymeric insulators behavior is using the concept of composite, inorganic particles were incorporated inside polymer matrix to produce what is called polymer composites [6, 7]. In the previous decade, the design

of composite materials involving either micro-scaled or nano-scaled inorganic and inorganic particles has gained great attention at power engineering to improve the properties of insulators dielectric, mechanical, and thermal [8-19]. The polymer composites were identified by their low working temperature, sensitivity to moisture and radiation also they have a high thermal expansion coefficient [20]. In many researches is seen that the particle type, size, weight, and surface of the polymer nanocomposites have an important role in its advantageous properties. Also, it is found that nanoparticles size introduced advantages over micron size because they increase the resistance to degradation and improve the thermo-mechanical properties without an unnoticeable decrease in dielectric strength [21, 22]. TiO₂ is inexpensive semiconductor have an excellent properties allow incorporation into polymeric matrices as adequate nanofiller to create new nanocomposites which have advanced behavior. TiO₂ nanoparticles were chosen in this research because of their semi-conductive nature which acts well as charge traps and they are readily available [23]. This study aims to discuss the effect of incorporating nonfunctionalized and functionalized TiO₂ with different ratios (0.5, 2, 3.5 and 5% wt/wt) inside the XLPE matrix by an industrial method and show it is an effect on the statistical characteristics of XLPE. To get optimum results, it is found that, the dispersion of nanoparticles within polymeric material should be homogeneously distributed, and this can be done by treat and modify the nanoparticles surfaces chemically using silane coupling agents. This treatment of nanoparticles is carried out to make a conversion of their hydrophilic (inorganic) character into a hydrophobic (organic) character which leads to eliminating nanoparticles agglomeration and enhancing their distribution inside polymers matrices [24-27]. Transmission Electron Microscopy (TEM) is used to define the size of TiO₂ nanoparticles. After preparation of XLPE/TiO₂ nanocomposites samples, the characterization can be studied with Field Emission Scanning Electron Microscopy (FE-SEM), thermal analysis and X-Ray Diffraction (XRD) techniques. Moreover, the dielectric properties such as dielectric strength, relative permittivity and loss tangent of the prepared samples were measured.

2. Experimental Setup

2.1. Material

CLNA-8141EHV is a crosslinked low-density polyethylene compound designed for extra high voltage power cable insulation that has a high degree of cleanliness was provided by El- Sewedy Electric Co., Egypt which has an extremely low level of contamination. Titanium Dioxide (TiO₂) nanoparticles were provided from sigma-Aldrich as titanium (IV) oxide CAS 13463-67-7, Mwt. 79.87, nanopowder, 99.5% purity. Methane sulfonic acid for surface activation of nanoparticles with 98% purity was purchased from LOBA Chemie. The coupling agent used is Gamma-amino propyltriethoxy silane abbreviated as "amino silane"

with purity 99% which was purchased from Momentive Inc. This study aims to discuss the effect of incorporating nonfunctionalized and functionalized TiO₂ inside the XLPE matrix using an industrial method. The size of the nanoparticles will be measured. The mechanical characteristics and the dielectric properties such as relative permittivity, loss tangent and dielectric strength will be measured.

2.2. Functionalization of Nanoparticle Materials

The surface modification is performed through two sequential steps. The first step is called "surface activation" of the nanoparticles with hydroxyl groups through the acid etching method. The second step is called "surface modification" for the activated nanoparticles using amino silane as a coupling agent. In the first step, 10 g of TiO₂ were stirred with 100 ml of 10% methane-sulfonic acid at 110°C for 4 hours. After that, the powder was collected using Hitachi centrifuge at 1500 rpm for 5 min and washed several times with de-ionized water then drying it for 24 hours at 120°C in a vacuum oven.

The second step is the functionalization of nanoparticles in which 3 g of the activated nanoparticles was added to 60 ml of toluene in a round flask for sonication in a water bath sonicator (Elmasonic, S-60H) for 30 min. at 70°C followed by stirring for 2 h at 500 rpm and 70°C. A solution of 10% (wt/wt) of amino silane in toluene was added dropwise and the stirring process was continued for 8 hours. Finally, the functionalized nanoparticles were collected and washed with isopropanol and dried in a vacuum oven at 120°C for 24 hours for further characterization [28-29].

2.3. Preparation of XLPE Nanocomposites

In our study, the XLPE/TiO₂ nanocomposites were prepared by the melt blending method which is the master batch method in the El-Sewedy Egy-tech laboratory. Each nanocomposite formulation consists of 150 g of XLPE pellets with different weights of either functionalized or nonfunctionalized TiO₂ nanoparticles (0.5, 2, 3.5 and 5% wt/wt). XLPE/TiO₂ sheets, with dimension 20×20 cm and 1.07 – 2.2 mm thicknesses were prepared by as following; XLPE pellets and nanoparticles were mixed at 150°C with 80 rpm for 15 min then annealed at 60°C for 24 hours. The mixture was blended in the two-roll mixer (Battaglion, MCC 150*300/R-o) at 150°C for 15 min, with 30 rpm. The sample was pressed at 150°C under 200 bars for 15 min using GDB-Laboratory hot/cold press (Gibit instruments Co.).

3. Characterization of Nanocomposites

3.1. Morphology Studies

The morphology and size of TiO₂ nanoparticles were studied using high-resolution Transmission Electron Microscope (TEM), the model type is (JEOL-JEM-2100). The images were recorded at a voltage of 120 kV.

3.2. Field Emission Scanning Electron Microscopy (FE-SEM)

Field Emission Scanning Electron Microscopy (FE-SEM) (Quanta FEG 250, FEI-Inc.) was utilized for surface morphology investigation for some selected samples. The microscope was attached to the energy dispersive X-ray analysis (EDX) unit. The images have been recorded at a voltage of 10–15 kV.

3.3. X-ray Diffraction (XRD)

The XRD patterns of XLPE/TiO₂ nanocomposites were investigated on a Diano X-ray diffractometer using CoK α radiation source energized at 45 kV and a Philips X-ray diffractometer (PW 1930 generator, PW 1820 goniometer) with CuK radiation source ($\lambda=0.15418$ nm), at a various angle range of 2θ between 10 to 80° in reflection mode.

3.4. Thermogravimetric Analysis (TGA)

The thermal stability for XLPE/TiO₂ nanocomposites has been tested by thermogravimetric analysis (TGA, Shimadzu DTG-60, Japan) STA 6000 Perkin Elmer Analyzer. The analysis were done between 25°C to 900°C and the heating rate was 10°C/min under argon.

3.5. Dielectric Properties

Relative permittivity and the loss factor were measured using Hioki 3532-50 LCR Hi Tester, frequency range of 1 Hz–1 MHz. The measurement of the breakdown strength was carried out using a sphere-to-sphere test cell energized from a test transformer (400V/250kV) according to ASTM (D149-09) standard. The measuring setup is modeled using a finite element method and the distribution of voltages and electric fields were determined in and around the different insulating samples.

3.6. Mechanical Properties

The mechanical properties such as elongation, and tensile

strength were measured by applying the tensile test using Plastic Micro-tensile Testing (ASTMD 1708-93 standards for micro tensile specimens). All mechanical properties are investigated at room temperature

4. Results and Discussions

4.1. TEM Specification of Nanoparticles

By using TEM, we can measure the size of the nanoparticles accurately. TiO₂ nanoparticles average size was about (60–280) nm as shown in Figure 1.

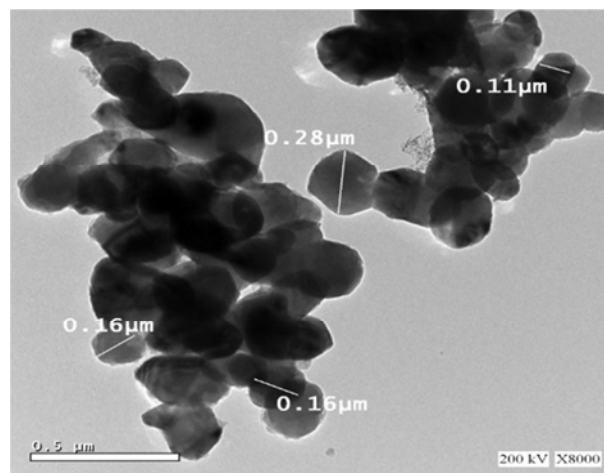


Figure 1. TEM micrographs of TiO₂ nanoparticles.

4.2. FE-SEM Micrographs of XLPE Nanocomposites

The surface morphology of the samples was analyzed using FE-SEM which can describe the microstructure dispersion of nanoparticles inside the polymer chains. FE-SEM micrographs for both cross-section area and the surface of all samples were carried out. Figure 2 shows the FE-SEM micrographs for both cross-section area and the surface of the XLPE without nanoparticles.

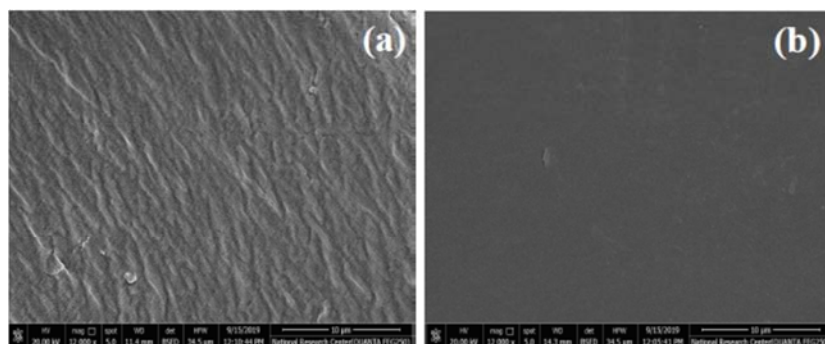


Figure 2. FE-SEM micrographs of (a) Cross-section area and (b) surface of the XLPE without nanoparticles.

The effect of amino silane surface treatments of TiO₂ nanoparticles on the dispersion of TiO₂ within the XLPE matrix can be achieved by comparing the FE-SEM micrographs for the cross-section area and the surface of the two nanocomposites one with nonfunctionalized and other with functionalized TiO₂ as shown in Figure 3.

It is clear that at the same addition ratio of TiO₂ there are some aggregates of TiO₂ with few micrometers in size within the nonfunctionalized TiO₂ but in case of functionalized TiO₂ there is a good dispersion and homogenous distribution for the nanoparticles in the composite, that is due to the chemical functionalization process of the TiO₂ nanoparticles surface lead

to strong interactions between nanoparticles and XLPE matrix.

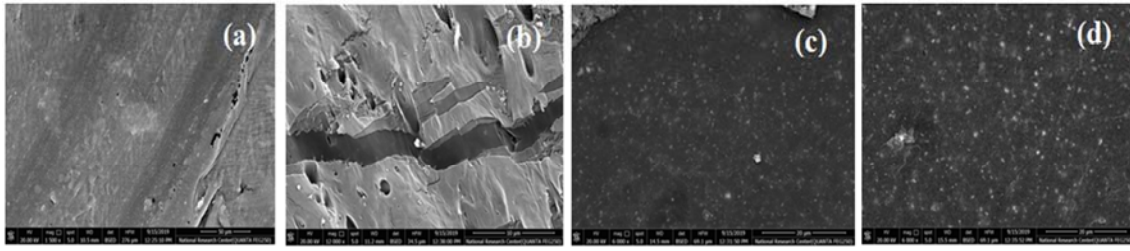
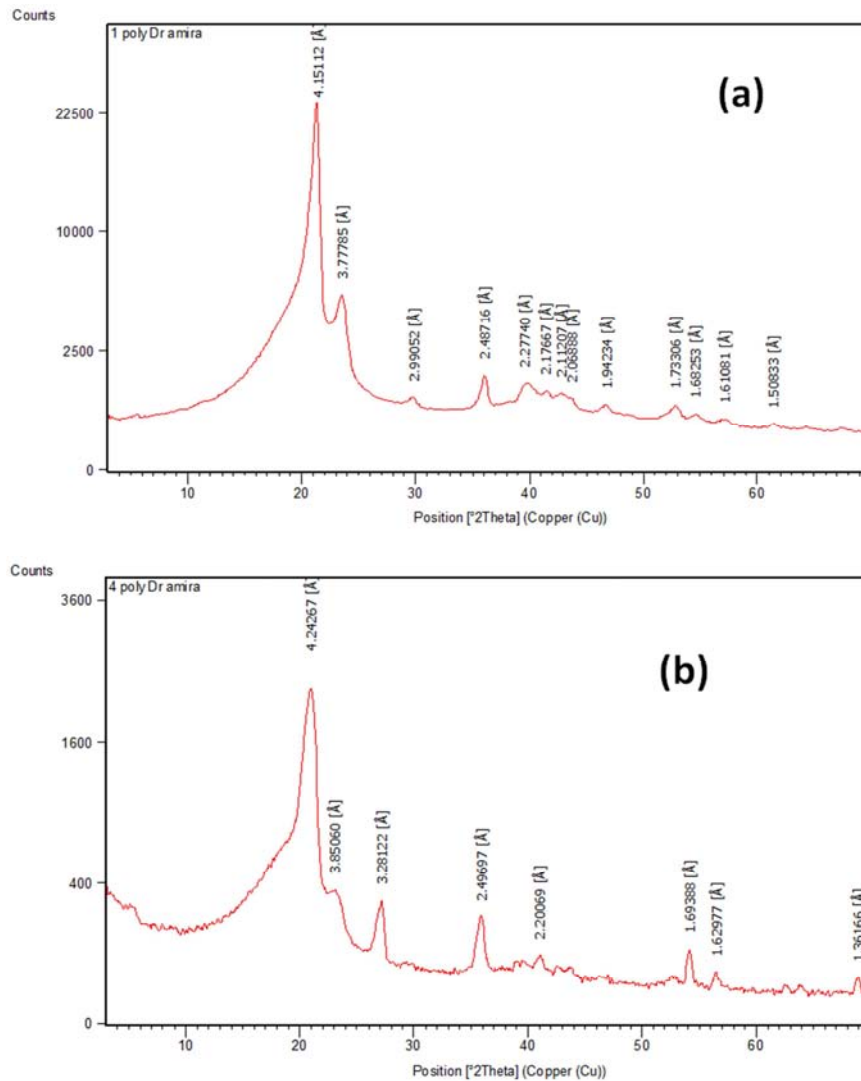


Figure 3. FE-SEM micrographs as cross section area and surface of XLPE/TiO₂ nanocomposites (a-c) with non-functionalized (b-d) and functionalized TiO₂.

4.3. X-ray Diffraction (XRD)

The X-ray diffraction pattern of the tested XLPE samples indicated an amorphous halo and two major crystalline peaks at $2\theta=21.40^\circ$ (d (interplanar distance)= 4.15112 \AA) and $2\theta=24.06^\circ$ ($d=3.777 \text{ \AA}$), Figure 4a, [30]. Other small peaks can be observed at $2\theta=29.8784^\circ$ ($d=2.99052 \text{ \AA}$), $2\theta=39.573^\circ$ ($d=2.27740 \text{ \AA}$), $2\theta=41.4867^\circ$ ($d=2.17667 \text{ \AA}$), $2\theta=42.8169^\circ$ ($d=2.11207 \text{ \AA}$), $2\theta=43.7564^\circ$ ($d=2.06888 \text{ \AA}$), $2\theta=46.7704^\circ$ ($d=1.94234 \text{ \AA}$), $2\theta=52.8265^\circ$ ($d=1.73306 \text{ \AA}$), $2\theta=54.5422^\circ$ ($d=1.68253 \text{ \AA}$), $2\theta=57.1883^\circ$ ($d=1.61081 \text{ \AA}$), and $2\theta=61.4206^\circ$ ($d=1.50833 \text{ \AA}$).

The major crystalline peaks at $2\theta=21.40$ and 24.06° did not change by the addition of TiO₂ to XLPE with small changes in the interplanar spacing which recorded a value not more than ($0.006 - 0.01 \text{ \AA}$) with an additional peaks at $2\theta=27.1779^\circ$ ($d=3.28122 \text{ \AA}$) and $2\theta=68.9025^\circ$ ($d=1.36166 \text{ \AA}$) in case of nonfunctionalized and $2\theta=27.3837^\circ$ ($d=3.25702 \text{ \AA}$) and $2\theta=68.9254^\circ$ ($d=1.36127 \text{ \AA}$) for functionalized XLPE/TiO₂ nanocomposites respectively which represents of crystallization of TiO₂ nanoparticles inside the polymer matrix (Figure 4b-c).



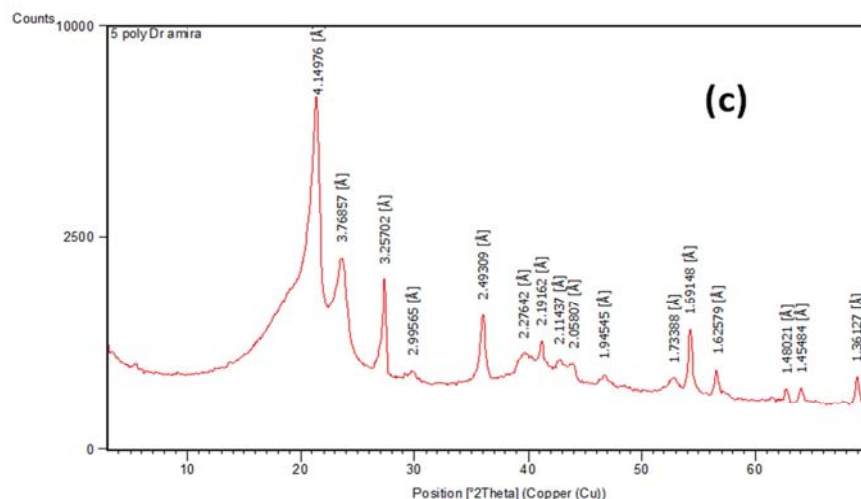


Figure 4. X-ray diffraction patterns of: (a) XLPE, (b) nanocomposites with nonfunctionalized, and (c) functionalized TiO_2 .

4.4. Thermo-gravimetric Analysis (TGA)

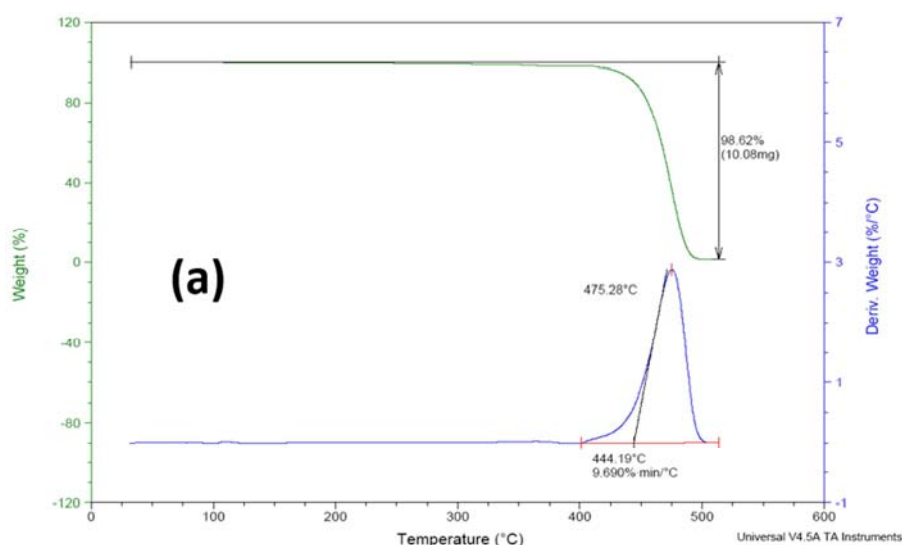
In TGA analysis, the rate of material weight is changing with varying temperature. The onset of time or temperature of the initial weight loss can be considered as a loss of volatiles, absorbed water or lower molecular weight constituents. The onset of irreversible weight loss could suggest the real thermal degradations [31]. Accordingly, the relative thermal stability of the nanocomposites has been evaluated by comparing their decomposition temperatures. In this study, the weight loss at 300°C, 400°C, and 475°C (decomposition temperature) are the main criteria used to indicate the thermal stability of nanocomposites. The higher the values of decomposition temperatures the higher the thermal stability of the nanocomposites will be [32].

From Figure 5 and Table 1, it is seen that the weight loss

of XLPE was 0.83, 1.99, and 62.9% at 300, 400, and 475°C. It means that, its rate of loss decreased with increasing temperature. By the addition of nonfunctionalized and functionalized TiO_2 nanoparticles the weight loss increased at 300 and 400°C while decreased at 475°C in case of functionalized TiO_2 . The decomposition temperature decreased with nonfunctionalized TiO_2 and increased with functionalized TiO_2 . This means the addition of functionalized nanoparticles into the XLPE matrix enhanced the thermal stability of XLPE. This may be due to that the higher thermal resistance of the inorganic filler which has an onset temperature of 580°C [33-36] or may be due to the lower mobility of the matrix chains as a result of the strong interaction between the nanoparticles and the XLPE matrix.

Table 1. Weight loss and decomposition temperatures of XLPE and XLPE/ TiO_2 nanocomposite.

Sample	Weight Loss (%)			Decomposition Temperature °C
	300°C	400°C	475°C	
XLPE	0.83	1.99	62.9	475.28
XLPE/ Nonfunctionalized TiO_2	1.02	2.34	64.07	474.7
XLPE/ Functionalized TiO_2	1.23	2.3	46.35	482.94



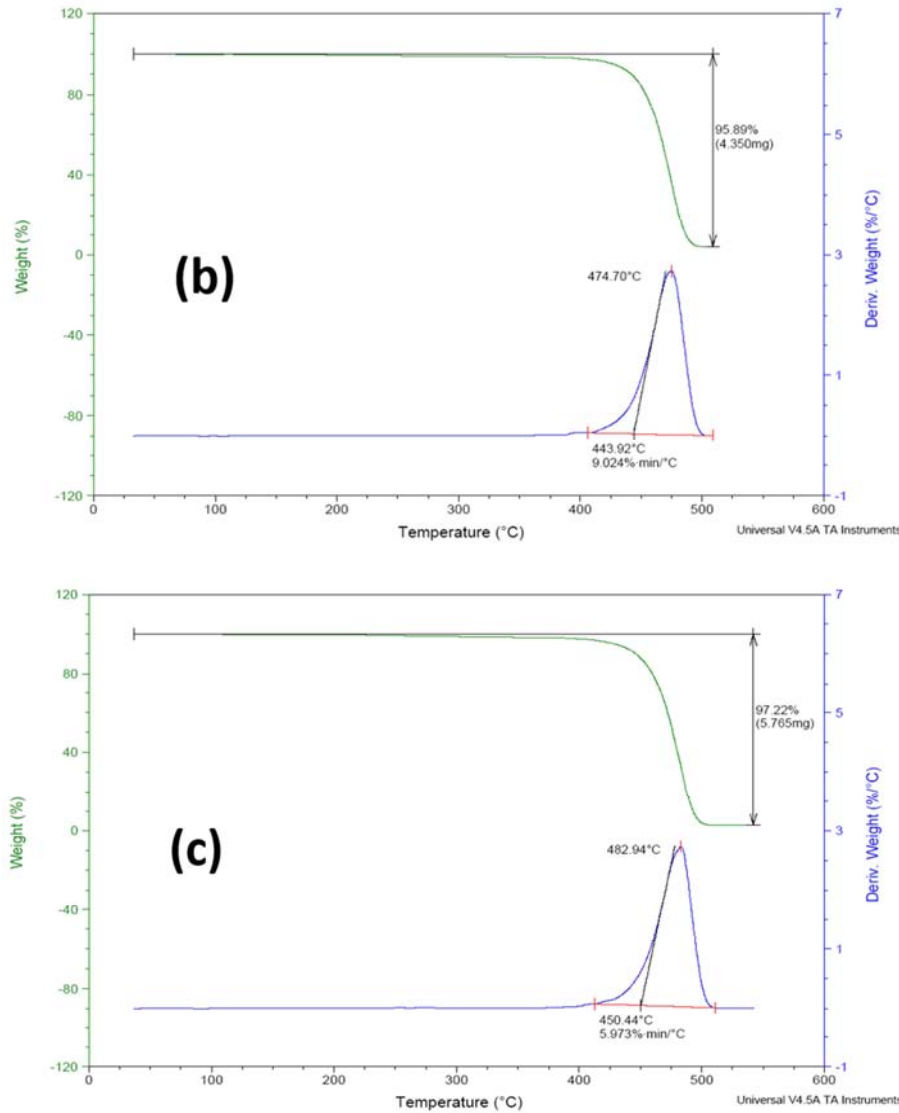


Figure 5. TGA of: (a) XLPE (b) XLPE nanocomposite with nonfunctionalized TiO₂ and (c) XLPE nanocomposite with functionalized TiO₂.

4.5. Dielectric Properties of XLPE Nanocomposites

The important dielectric properties, such as the relative permittivity, dielectric loss ($\tan \delta$) and the dielectric strength were measured. These three parameters measure the quality of the dielectric material used as insulation in HV applications.

4.5.1. Relative Permittivity and Dielectric Loss

The relative permittivity and the dielectric loss of the nonfunctionalized and amino-functionalized XLPE/TiO₂ nanocomposites samples were investigated. Figure 6 and Figure 7 show the variation of relative permittivity (ϵ_r) and dielectric loss ($\tan \delta$) of XLPE and XLPE/TiO₂ nonfunctionalized and functionalized nanocomposites admixed with various amounts of nanoparticles.

It can be concluded that in most samples, with increasing the frequency the dipoles do not have enough time to be created in the direction of the electric field. So, the samples did not present high polarizability in high frequencies regions, which leads to a reduction in the relative permittivity values.

However, and in contrast, when the frequency decreases, the time scales will increase and most mobile atom groups begin to orient, resulting in an increase in the observed values of ϵ_r . Also, it is observed that all prepared samples have relatively high $\tan \delta$ values at low frequencies, and this is may be attributed to the higher leakage current in the system.

Figure 6a and 7a show that the values of permittivity of the nanocomposites are varied with the concentration of TiO₂ and XLPE/TiO₂ sample with 2 wt.% have the lowest ϵ_r values especially with the functionalized sample which decreases by about 3.1% at power frequency 50 Hz. This may be due to the restriction in the polymer chain mobility due to good incorporation and dispersion of the functionalized TiO₂ nanoparticles within these chains. This indication of the chemical functionalization of TiO₂ assists their dispersion and enhances their compatibility with the polymeric matrix.

Also, it is obvious that both XLPE/TiO₂ nonfunctionalized and amino-functionalized nanocomposites with 5 wt.% have higher ϵ_r values than both neat XLPE since they increased by 15.46% and 2.061% respectively at power frequency 50 Hz.

This increase may be due to the reduction in the interface interaction area between the polymer matrix and nanoparticles that results from nanoparticle agglomeration. These agglomerated nanoparticles may act as voids between the polymer chains and facilitate their mobility, and hence account for more molecular polarization.

Figure 6b and 7b show the curves of dielectric loss, $\tan \delta$, versus frequencies for different concentration of TiO_2 nanocomposites. The figures indicated that XLPE/ TiO_2 nanocomposites have high dielectric losses at low frequencies, which may be attributed to the high leakage current in the test system. At the same time, it can be noticed that $\tan \delta$ of all XLPE/ TiO_2 samples recorded lower values than XLPE specimen. Also, the amino-functionalized XLPE/ TiO_2 samples have lower values of $\tan \delta$ than nonfunctionalized ones at frequencies up to 1000 Hz. Clearly, at high frequencies, the $\tan \delta$ values were not affected by increasing the amount of TiO_2 nanoparticles. The obtained results indicated that at power frequency (50 Hz), the

dielectric losses for 2 wt.% nonfunctionalized XLPE/ TiO_2 sample is reduced by 27.34% over the neat XLPE, which considers the lowest improvement case, and $\tan \delta$ at 5 wt.% amino-functionalized XLPE/ TiO_2 sample is reduced by 91.59%, which shows a great improvement, Table 2.

Table 2. Permittivity and dielectric loss of XLPE and XLPE/ TiO_2 nanocomposites at 50 Hz.

Sample	Wt. %	Relative permittivity (ϵ_r)	Loss Factor ($\tan \delta$)
XLPE	0	2.91	0.0113
XLPE / Nonfunctionalized TiO_2	0.5	2.94	0.0081
	2	3.13	0.00821
	3.5	3.1	0.00292
	5	3.36	0.00189
	0.5	2.91	0.00276
XLPE/ Functionalized TiO_2	2	2.82	0.00190
	3.5	2.94	0.00138
	5	2.97	0.00095

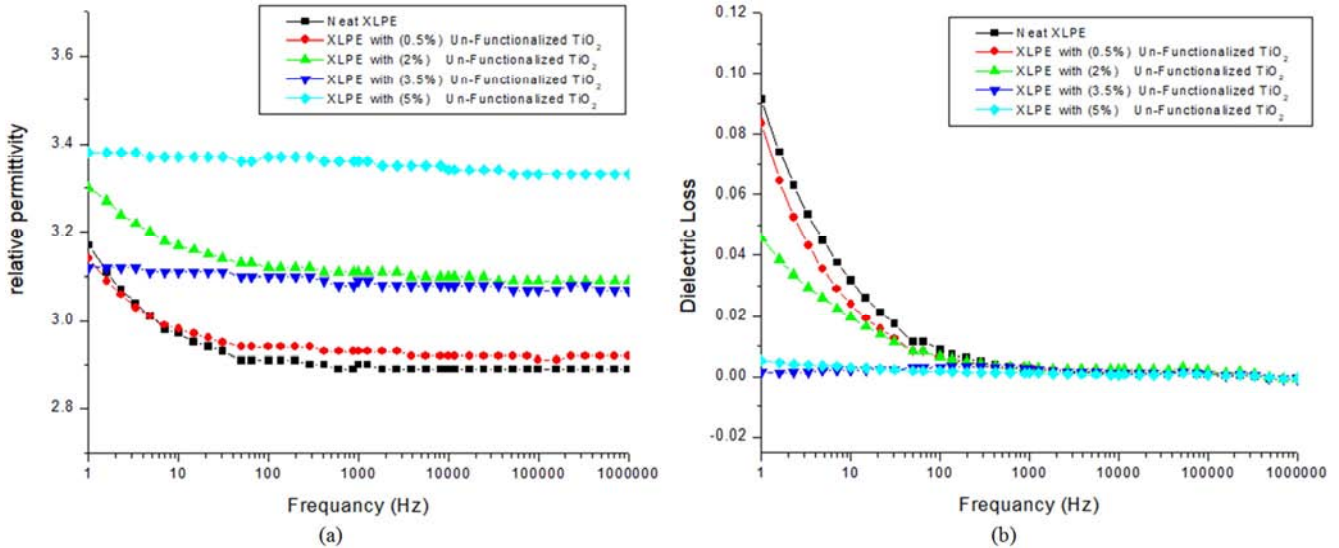


Figure 6. XLPE and nonfunctionalized XLPE/ TiO_2 nanocomposites (a) Relative permittivity, (b) dielectric loss.

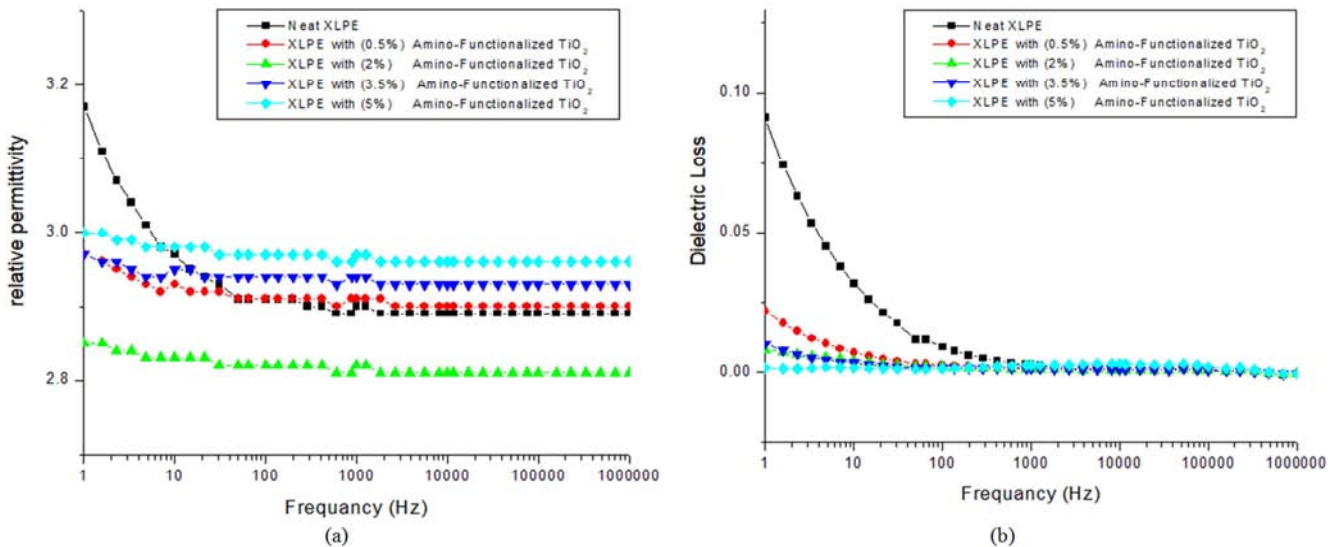


Figure 7. XLPE and amino-functionalized XLPE/ TiO_2 nanocomposites (a) Relative permittivity, (b) dielectric loss.

4.5.2. AC Breakdown Strength

The AC breakdown voltages (AC-BDV) of XLPE/TiO₂ nanocomposites were measured. Table 3 shows the measured values of AC breakdown strength of functionalized XLPE/TiO₂ and the nonfunctionalized XLPE/TiO₂ and the percentage of enhancement. The table shows that the functionalized XLPE/TiO₂ nanocomposites are higher than that of the nonfunctionalized ones. This can be attributed to the creation of a strong interfacial area between nanoparticles and the polymeric matrix. In addition, by increasing the addition ratio of nanofiller, the AC-BDS is increased, except at weight fractions of 3.5 wt.% and 5 wt.% of TiO₂ nanoparticles, the AC-BDS began to reduce. The addition of TiO₂ into the XLPE matrix can increase the AC-BDS, while with a high concentration of nanoparticles a lot of agglomeration maybe produced and cause a reduction in AC-BDS. Moreover, the maximum measured values of AC-BDS are happen in the samples of XLPE/TiO₂ with 2 wt.% and 3.5 wt.% amino-functionalized TiO₂ nanocomposites as shown in Figure 8, which are enhanced by 24.5% and 20.08%,

respectively, over XLPE. Otherwise, for nonfunctionalized samples, there is no enhancement was observed.

The AC-BDS was obtained using a simulation model on Femm package, which uses the finite element method in 2-dimensional pattern (i.e. an axisymmetric form). The voltage applied to the upper sphere is the breakdown voltage taken from the experimental result, and the lower sphere is grounded. The voltage and electric field distribution inside and around the samples are traced and evaluated. The breakdown strength at the tip point of the HV sphere was recorded as in a Table 3, in case of XLPE/nonfunctionalized TiO₂ and XLPE/amino-functionalized TiO₂ nanocomposites. The electric potential and electrostatic field distribution in and around the sample are shown in Figure 9a and Figure 9b for XLPE nanocomposite with 2 wt.% amino-functionalized nanoparticles. It is shown that there is a high agreement between the measured and the simulated results, where the maximum enhancement of simulation results happened at 2 wt.% amino-functionalized XLPE/TiO₂ sample.

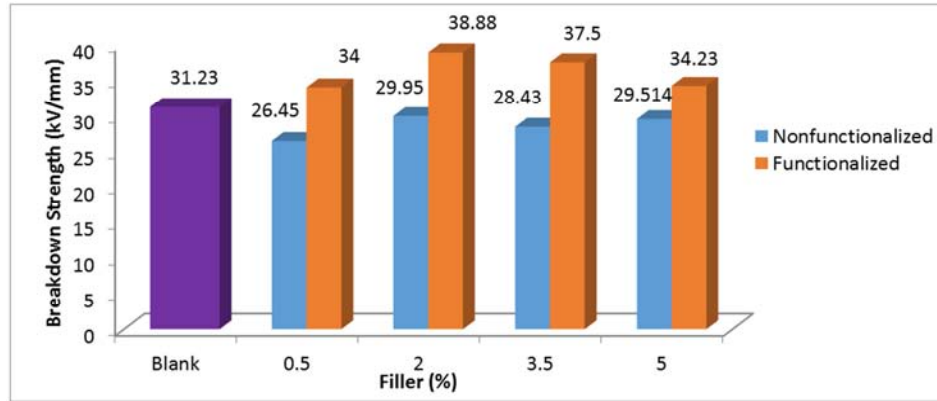


Figure 8. AC-BDS rms values of XLPE/TiO₂ nanocomposites.

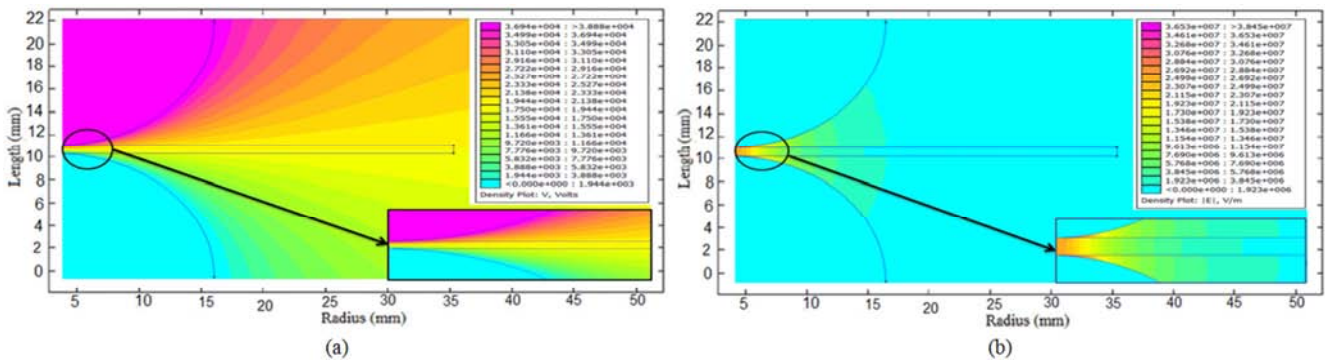


Figure 9. (a) AC potential distribution around sphere electrode and along with sample thickness, (b) Electrostatic field distribution inside 2 wt.% XLPE/amino-functionalized TiO₂ nanocomposite for the sphere to sphere configuration.

Table 3. Measured and simulated rms values of AC-BDS of the XLPE/TiO₂ nanocomposites at sphere-sphere field.

Sample	Wt. (%)	Breakdown strength (kV/mm)	Improvement (%)	Simulated Breakdown strength (kV/mm)
XLPE	0	31.23	0	32.64
XLPE/ Nonfunctionalized TiO ₂	0.5	26.45	-15.30%	27.6
	2	29.95	-4.10%	31.46
	3.5	28.43	-8.97%	30.03
	5	29.514	-5.49%	30.096

Sample	Wt. (%)	Breakdown strength (kV/mm)	Improvement (%)	Simulated Breakdown strength (kV/mm)
XLPE/ Functionalized TiO ₂	0.5	34	8.87%	35.108
	2	38.88	24.50%	40.401
	3.5	37.5	20.08%	38.76
	5	34.23	9.61%	35.49

4.6. Mechanical Properties

Tensile strength and elongation level measurement was carried for XLPE with nonfunctionalized and functionalized TiO₂ at different wt.%. Figure 10 shows tensile strength for XLPE was 10 MPa and 584 elongations. For nonfunctionalized XLPE/TiO₂ nanocomposites, it can be ascertained from the Figure 10 that the tensile strength is increased with increasing the wt.% and the maximum value was at 3.5% wt. which reaches 11.6 MPa and the elongation was 450, then with increasing the wt.%, tensile strength decreases reaching 10.5 MPa at 5 wt.% and 394 in elongation. This behavior can be explained as follow, in case of high loading of nonfunctionalized TiO₂, the agglomeration of the nanoparticles acts as relatively large voids in the tested sample which make the molecular chains moving freely and slipping past one another

For functionalized XLPE/TiO₂ nanocomposites, it can be

ascertained that the tensile strength is maximum at 3.5 wt.% which reaches 12.4 MPa and the elongation value was 460% then with increasing the wt.%, tensile strength decreases reaching 11 MPa at 5 wt.% with elongation 402%. When compare to blank sample, 3.5 wt.% of functionalized titanium dioxide has more tensile strength and more elongation. These results emphasis that TiO₂ functionalized nanoparticles improved the mechanical characteristics of XLPE sample. Such behavior in mechanical properties and the increase in the tensile strength with low loading of nanoparticle are resulted from their high specific surface available for interactions with the polymer matrix. For many polymers, addition of nanofiller causes a notable diminution of chain elongation, this could be attributed to the constraint of the chains mobility generated by creating a bonding between nanoparticles and polymer chains [37].

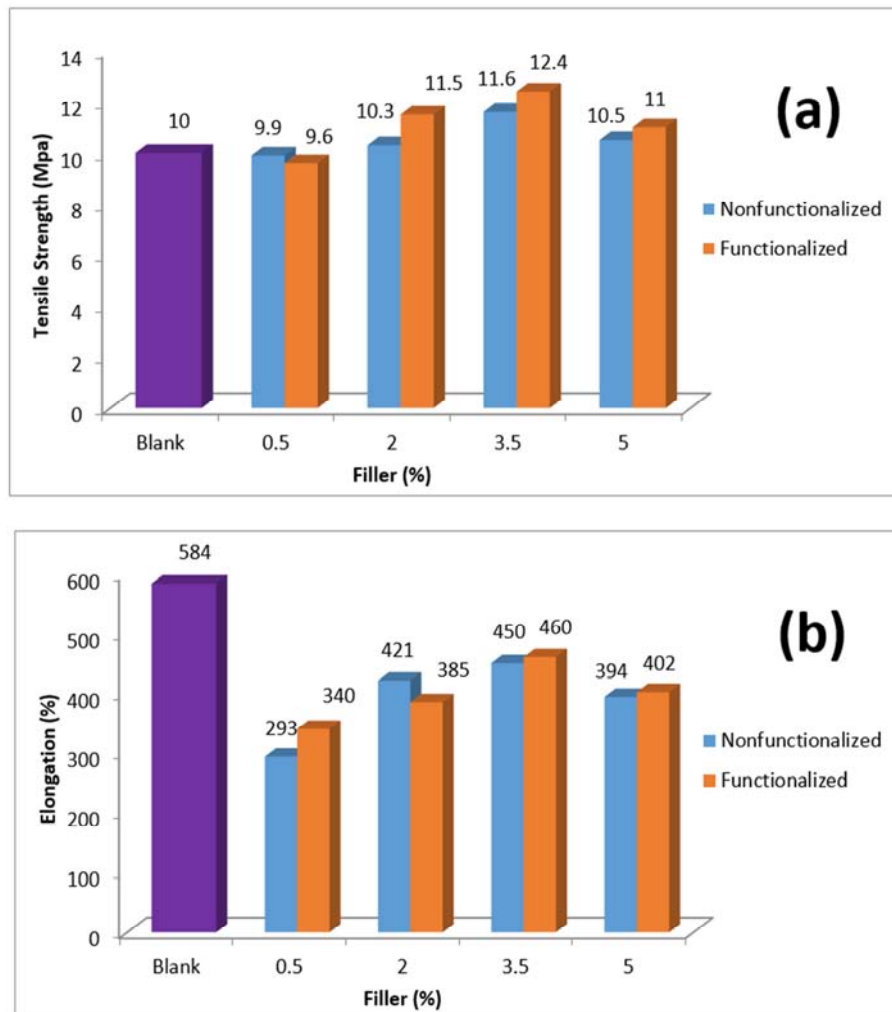


Figure 10. Tensile strength (a), and elongation (b) of nonfunctionalized and functionalized TiO₂/XLPE nanocomposites with different weight ratios.

5. Conclusion

The addition of inorganic nanoparticles into the XLPE matrix enhanced the thermal and mechanical properties of XLPE. The functionalization nanoparticles lead to an excellent dispersion within polymer chains. An improvement in relative permittivity and loss tangent, where the loss tangents for all XLPE/TiO₂ nanocomposites were less than that of the XLPE. The dielectric loss has a higher value in the low-frequency regions, where the interface polarization in XLPE nanocomposites is significant. The breakdown strength of the modified nanocomposites has higher values compared to blank (neat XLPE). As the percentage weight of nanoparticles increased, the interparticle distance decreases, which leads to a hindrance in charge carriers transferring and create a strong bond, which resulted in increasing the dielectric strength. However, it is noticed that more addition of TiO₂ nanoparticles decreases the dielectric strength and that's maybe due to the high concentration of nanoparticles leads to more agglomeration causing much reduction in AC-BDS.

References

- [1] King, A., Wentworth, V. H.: Raw materials for electric cables. Benn (1954).
- [2] Maddah Hisham, A.: Polypropylene as a promising plastic. A review. *Am. J. Polym. Sci.* 6, 1-11 (2016).
- [3] Hyvonen, P.: Prediction of insulation degradation of distribution power cables based on chemical analysis and electrical measurements. *Teknillinen korkeakoulu* (2008).
- [4] Hanley, T. L., Burford, R. P., Fleming, R. J., Barber, K. W.: A general review of polymeric insulation for use in HVDC cables. *IEEE Electrical Insulation Magazine*. 19, 13-24 (2003).
- [5] Tamboli, S. M., Mhaske, S. T., Kale, D. D.: Crosslinked polyethylene (2004).
- [6] Rajput, N.: Methods of preparation of nanoparticles-a review. *Inter. J. Adv. Engin and Tech.* 7, 1806 (2015).
- [7] Jeon, I. Y.; Baek, J. B. Nanocomposites derived from polymers and inorganic nanoparticles. *Materials*. 3, 3654-3674. (2010)/
- [8] Abdel-Gawad, N. M., El Dein, A. Z., Mansour, D. E. A., Ahmed, H. M., Darwish, M. M. F., Lehtonen, M.: Multiple enhancement of PVC cable insulation using functionalized SiO₂ nanoparticles based nanocomposites. *Electric Power Systems Research*. 163, 612-625 (2018)
- [9] Abdel-Gawad, N. M., El Dein, A. Z., Mansour, D. E. A., Ahmed, H. M., Darwish, M. M. F., Lehtonen, M.: Enhancement of dielectric and mechanical properties of polyvinyl chloride nanocomposites using functionalized TiO₂ nanoparticles. *IEEE Transactions on Dielectrics and Electrical Insulation*. 24, 3490-3499 (2017).
- [10] Abdel-Gawad, N. M., El Dein, A. Z., Mansour, D. E. A.; Ahmed, H. M., Darwish, M. M. F., Lehtonen, M.: Development of industrial scale PVC nanocomposites with comprehensive enhancement in dielectric properties. *IET Sci, Measurement and Tech.* 13, 90-96 (2018).
- [11] Qingyue, Y., Xiufeng, L., Peng, Z., Peijie, Y., Youfu, C.: Properties of Water Tree Growing in XLPE and composites, *International Conference on Electrical Materials and Power Equipment. (ICEMPE). IEEE.* 409-412 (2019)
- [12] Salh S. H., Raswl D. A.: Thermal stability of polymer composite films based on polyvinyl alcohol doped with different fillers. *Open Access Journal of Physics*. 2, 5-10 (2018).
- [13] Awad A. H., El-Wahab, A. A. A., El-Gamsy, R., Abdel-latif, M. H.: A study of some thermal and mechanical properties of HDPE blend with marble and granite dust. *Ain Shams Engineering Journal*. 10, 353-358 (2019).
- [14] Giżyński, M., Romelczyk-Baishya, B.: Investigation of carbon fiber-reinforced thermoplastic polymers using thermogravimetric analysis. *Journal of Thermoplastic Composite Materials*. 1-15 (2019).
- [15] Zhang, C., Chang, J., Zhang, H., Li, C., Zhao, H. Improved Direct Current Electrical Properties of Crosslinked Polyethylene Modified with the Polar Group Compound. *Polymers*. 11, 1624 (2019).
- [16] Liu, S. H., Shen, M. Y., Kuan, C. F., Kuan, H. C., Ke, C. Y., Chiang, C. L.: Improving Thermal Stability of Polyurethane through the Addition of Hyperbranched Polysiloxane. *Polymers*. 11, 697 (2019).
- [17] Liu, Z., Tu, R., Liao, Q., Hu, H., Yang, J., He, Y., Liu, W.: High thermal conductivity of flake graphite reinforced polyethylene composites fabricated by the powder mixing method and the melt-extruding process. *Polymers*. 10, 693 (2018).
- [18] Chi, X., Cheng, L., Liu, W., Zhang, X., Li, S.: Characterization of polypropylene modified by blending elastomer and nano-silica. *Materials*. 11, 1321 (2018).
- [19] Helal, E., Pottier, C., David, E., Fréchette, M., Demarquette, N. R. E.: Polyethylene/thermoplastic elastomer/Zinc Oxide nanocomposites for high voltage insulation applications: Dielectric, mechanical and rheological behavior. *European Polymer Journal*. 100, 258-269 (2018).
- [20] Gong, J., Hosaka, E., Sakai, K., Ito, H., Shibata, Y., Sato, K., Hamada, K.: Processing and thermal response of temperature-sensitive-gel (TSG)/polymer composites. *Polymers*. 10, 486 (2018).
- [21] Khan, I., Saeed, K., Khan, I.: Nanoparticles: Properties, applications and toxicities. *Arabian Journal of Chemistry*. 12, 908-931 (2019).
- [22] Khodaparast, P., Ounaies Zoubaida.: On the impact of functionalization and thermal treatment on dielectric behavior of low content TiO₂ PVDF nanocomposites. *IEEE Transactions on Dielectrics and Electrical Insulation*. 20, 166-167 (2013).
- [23] Kubacka, A., Fernández-García, M., Cerrada, M. L., Fernández-García, M.: Titanium Dioxide-Polymer Nanocomposites with Advanced Properties. In: *Nano-Antimicrobials*. Springer, Berlin, Heidelberg. 119-149 (2012).

- [24] Dalod, A. R., Henriksen, L., Grande, T., Einarsrud, M. A.: Functionalized TiO₂ nanoparticles by single-step hydrothermal synthesis, the role of the silane coupling agents. *Beilstein journal of nanotechnology*. 8, 304-312 (2017).
- [25] Chuang, W., Geng-sheng, J., Lei, P.; Bao-lin, Z., Ke-zhi, L., Jun-long, W.: Influences of surface modification of nano-silica by silane coupling agents on the thermal and frictional properties of cyanate ester resin. *Results in Physics*. 9, 886-896 (2018).
- [26] Zhao, J., Milanova, M., Warmoeskerken, M. M., Dutschk, V.: Surface modification of TiO₂ nanoparticles with silane coupling agents. *Colloids and surfaces A. Physicochemical and engineering aspects*. 413, 273-279 (2012).
- [27] Prado, L. A., Sriyai, M., Ghislandi, M., Barros-Timmons, A., Schulte, K.: Surface modification of alumina nanoparticles with silane coupling agents. *Journal of the Brazilian Chemical Society*. 21, 2238-2245 (2010).
- [28] A bdel-Gawad, N. M., Mansour, D. E. A., El Dein, A. Z., Ahmed, H. M., Darwish, M. M. F.: Effect of functionalized TiO₂ nanoparticles on dielectric properties of PVC nanocomposites used in electrical insulating cables. In *Eighteenth International Middle East Power Systems Conference (MEPCON)*. IEEE. 693-698 (2016).
- [29] Ahn, S. H., Kim, S. H., Lee, S. G.: Surface-modified silica nanoparticle-reinforced poly (ethylene 2, 6-naphthalate), *Journal of Applied Polymer Science*. 94, 812-818 (2004).
- [30] Hedir, A., Moudoud, M., Lamrous, O., Rondot, S., Jbara, O., Dony, P.: Ultraviolet radiation aging impact on physicochemical properties of crosslinked polyethylene cable insulation, *J. applied polymer sci.* 137, 48575 (2020).
- [31] Juliana, N. C., Chibuike, N. A. O., Josiah, E. A.: Evaluation of the Thermal Stability of Poly (O-phenylenediamine) (PoPD) by Thermogravimetric Analysis (TGA). *American J. Nanosci.* 5, 18-22 (2019).
- [32] El-Sayed, N. S., El-Sakhawy, M.; Hesemann, P., Brun, N., Kamel, S.: Rational design of novel water-soluble ampholytic cellulose derivatives. *Inter. J. biol. Macromol.* 114, 363-372 (2018).
- [33] Huang, C., Qian, X., Yang, R.: Thermal conductivity of polymers and polymer nanocomposites. *Materials Science and Engineering, R: Reports*. 132, 1-22 (2018).
- [34] Khan, H., Amin, M., Ali, M., Iqbal, M., Yasin, M.: Effect of micro/nano-SiO₂ on mechanical, thermal, and electrical properties of silicone rubber, epoxy, and EPDM composites for outdoor electrical insulations. *Turkish Journal of Electrical Engineering & Computer Sciences*. 25, 1426-1435 (2017).
- [35] Corcione, C. E., Frigione, M.: Characterization of nanocomposites by thermal analysis. *Materials*. 5, 2960-2980. (2012).
- [36] Nabinejad, O., Sujan, D., Rahman, M. E., Davies, I. J.: Determination of filler content for natural filler polymer composite by thermogravimetric analysis. *J. Thermal Analas. And Calorim.* 122, 227-233 (2015).
- [37] Q. OYU, A. P. S. SELVADURA: Mechanical behaviour of a plasticized PVC subjected to ethanol exposure. *Polymer degradation and stability*. 89 (1), 109-124 (2005).